

## Research Article

# Substitutions with Vanishing Rotationally Invariant First Cohomology

**Juan García Escudero**

*Facultad de Ciencias Matemáticas y Físicas, Universidad de Oviedo, 33007 Oviedo, Spain*

Correspondence should be addressed to Juan García Escudero, [jjge@uniovi.es](mailto:jjge@uniovi.es)

Received 17 November 2011; Accepted 5 December 2011

Academic Editor: Bo Yang

Copyright © 2012 Juan García Escudero. This is an open access article distributed under the Creative Commons Attribution License, which permits unrestricted use, distribution, and reproduction in any medium, provided the original work is properly cited.

The cohomology groups of tiling spaces with three-fold and nine-fold symmetries are obtained. The substitution tilings are characterized by the fact that they have vanishing first cohomology group in the space of tilings modulo a rotation. The rank of the rational first cohomology, in the tiling space formed by the closure of a translational orbit, equals the Euler totient function evaluated at  $N$  if the underlying rotation group is  $\mathbb{Z}_N$ . When the symmetries are of crystallographic type, the cohomologies are infinitely generated.

## 1. Introduction

The computation of topological invariants of tiling spaces  $\Omega$  is a subject of increasing research activity, mainly since the work of Anderson and Putnam [1].

We use substitution rules to define collections of tilings. The expanding hierarchical structures that arise are essentially the same at each level, because they are described by a single substitution map. More general formalisms for handling general spaces of hierarchical tilings are studied in [2].

The simplest invariants of tiling spaces are the Čech cohomology groups. A relevant fact, also from the point of view of applications, is that the Čech cohomology is related to the gap distribution in the spectrum of the Schroedinger operator with a potential associated to a particular tiling. The Čech cohomology groups may be interpreted also in terms of certain tiling properties. For projection tilings, there is in the first cohomology at least a subgroup isomorphic to the reciprocal lattice of the tiling [3], and hence for a tiling with  $N$ -fold symmetry its minimal dimension is given by the Euler totient function  $\Phi(N)$ . If the stretching factor of a one-dimensional substitution tiling is a Pisot number of algebraic degree  $k$  and the rank of the first rational Čech cohomology is also  $k$ , then the number of appearances of a

patch in a return word is determined by the Euclidean length of the return word [4]. Based on this results, it has been shown in [5] that the top-dimensional cohomology for a tiling in  $\mathbf{R}^d$  governs patch frequencies and the number of appearances of a patch in a finite region.

A class of tiling spaces with fivefold symmetry has been analyzed in [6]. The rank of the first cohomology coincides with  $\Phi(5)$  and its restriction in the space of tilings modulo a fivefold rotation is zero. In this paper we study several examples of tiling spaces with crystallographic and noncrystallographic symmetries with analogous properties. They have vanishing first cohomology in the space of tilings modulo a rotation  $\bar{\Omega}$ . When the integer first cohomology in  $\Omega$  is finitely generated, as in the tilings with ninefold and pentagonal symmetries, its rank coincides with the Eulers totient function. In the cases with crystallographic symmetries, it is the rank of the rational first cohomology which equals the Eulers totient function.

## 2. Geometric Constructions of Substitution Tilings with $d$ -Fold Symmetry and Algebraic Surfaces

An extension of the methods introduced in [7] for tilings with odd symmetries nondivisible by three to all the symmetries has been given in [8]. There are four types of geometric constructions consisting in straight lines in  $d$  orientations: (A) for  $d = 2m$ , (B) for  $d = 2m + 1$ , (C) for  $d = 6m$ , and (D) for  $d = 6m + 3$ . They produce simplicial arrangements  $S_X, X = A, B, C, D$ , which are the basis for the generation of planar tilings with arbitrarily high symmetry. The systems with  $d$  odd are included in the systems with  $d$  even: (B) is included as a subsystem of (A), and (D) is included in (C). The fact that, in general, a system with  $d$  lines is included in another with  $2d$  lines allows to introduce in a systematic way arrows on the edges, which are necessary for the definition of the inflation rules generating face-to-face tilings [6]. We give an alternative formulation which simplifies the construction. Systems of lines, equivalent up to scaling, translation, and rotation, to those obtained with the constructions (A) and (B) are  $\{\Lambda_{k,d}(x, y, 0) = 0\}$ ,  $k = 1, 2, \dots, d$ , where

$$\Lambda_{k,d}(x, y, \tau) := y - \left( \cos\left(\frac{k2\pi}{d}\right) - x \right) \tan\left(\frac{k\pi}{d} + \tau\right) - \sin\left(\frac{k2\pi}{d}\right) \quad (2.1)$$

The simplicial arrangements  $S_C, S_D$  and their mirror images  $\bar{S}_C, \bar{S}_D$  can be obtained also by using  $\Lambda_{k,d}(x, y, \tau)$  for certain values of  $\tau$ . For fixed  $d$  we consider the subset formed by the lines  $\Lambda_{2k-1,2d}(x, y, \tau)$  with  $k = 1, 2, \dots, d$  and  $\tau = n\pi/4d$ . When  $d = 3m$ , we get, for  $n = 0, 1, 2, \dots, 8d$ , successive rotations of two types of simple arrangements of lines (no more than two lines intersect)  $\Sigma_1, \Sigma_2$  and the two types of simplicial arrangements  $S_A, S_C$  and  $S_B, S_D$  for  $d$  even and odd, respectively. In addition to the nontriangular shapes,  $\Sigma_1, \Sigma_2$ , have two sets of triangular prototiles:  $\Sigma_1$  has the prototiles of  $S_A, S_B$  while  $\Sigma_2$  and its mirror image  $\bar{\Sigma}_2$  have the prototiles of  $S_C, S_D$  and  $\bar{S}_C, \bar{S}_D$ . In Figure 1(a) we show the case  $d = 5$  with (from top to bottom)  $n = 0, 1, 2, \dots, 6$ . Two rotated versions of  $S_B$  correspond to  $n = 2, 6$ , the others are simple arrangements of lines  $\Sigma_1$  obtained when  $n = 0, 4$ . The case  $d = 6$  with  $n = 0, 1, 2, \dots, 6$  can be seen in Figure 1(b). Now we have two simplicial arrangements:  $S_C$  with 3 prototiles when  $n = 2$  and  $S_A$  with one prototile for  $n = 6$ . When  $n = 0$ , the simple arrangement  $\Sigma_1$  has 6 copies of the prototile appearing in  $S_A$ , and when  $n = 4$ ,  $\Sigma_2$  has seven triangles with 3

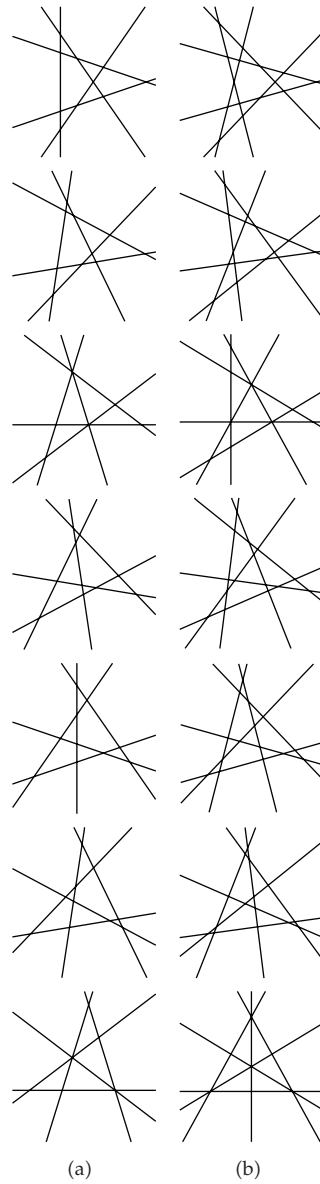


**Figure 1:** Line configurations described by (2.1) for (from top to bottom) (a)  $d = 5$ ;  $n = 0(\Sigma_1), 1, 2(S_B), 3, 4(\Sigma_1), 5, 6(S_B)$  and (b)  $d = 6$ ;  $n = 0(\Sigma_1), 1, 2(S_C), 3, 4(\Sigma_2), 5, 6(S_A)$ .

different shapes (prototiles in  $S_C$ ). In both cases the prototiles have edges with three different lengths as in Section 4.

The line configurations for  $d = 9$  can be seen in Figure 2(a) when  $n = 0, 1, 2, 3$  and Figure 2(b) for  $n = 4, 5, 6$ . We get  $\Sigma_1$  when  $n = 0, 12$ , while  $\Sigma_2$  and  $\bar{\Sigma}_2$  are obtained with  $n = 4, 8$ . The simplicial arrangement  $S_B$  corresponds to  $n = 6$  and we get  $S_D, \bar{S}_D$  when  $n = 2, 10$ . By using the notation in [9], the prototiles appearing in  $\Sigma_1$  and  $S_B$  are  $a, b, c$  (we use capital letters in Section 3 to describe the same tiles), while in  $\Sigma_1$  and  $S_D$  there are seven prototiles  $a, b, c, d, e, f, g$ . All the prototiles now have edges with four different lengths as in Section 3.

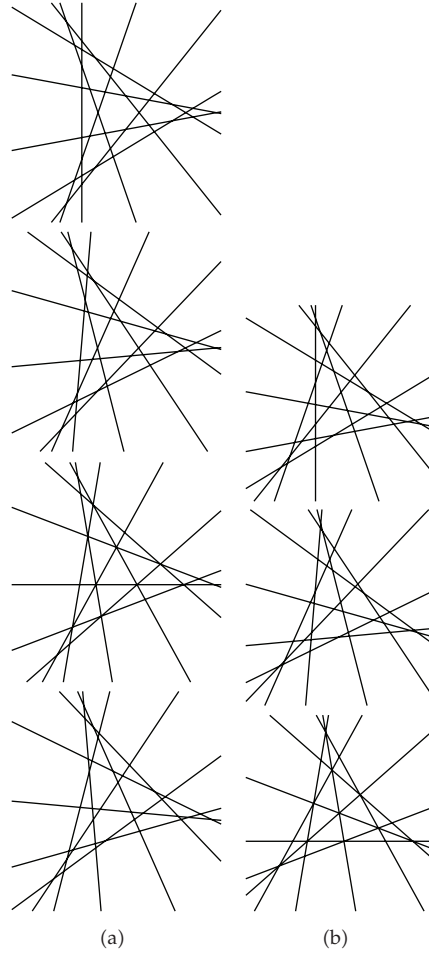


**Figure 2:** Simple and simplicial arrangements for  $d = 9$  (a)  $n = 0(\Sigma_1), 1, 2(S_D), 3$ , (b)  $n = 4(\Sigma_2), 5, 6(S_B)$ .

The simple arrangements  $\Sigma_1, \Sigma_2$  are on the basis of a construction of algebraic surfaces with many real nodes proposed recently [10]. The surfaces have affine equations  $S(x, y, z) := F(x, y) + \lambda F(z, 0) + \mu = 0, \lambda, \mu \in \mathbf{R}$ , where the plane curve  $F(x, y)$  is a product of lines corresponding to a simple arrangement. Real variants of Chmutov surfaces [11] are based on  $\Sigma_1$  as shown in [12]. On the other hand  $\Sigma_2$ , and its mirror image  $\bar{\Sigma}_2$ , have one more triangle than  $\Sigma_1$ , and this property can be used to construct surfaces with more singularities. The dynamical formulation of the line configurations given by (2.1) can then be used to get deformations of the surfaces by varying  $\tau$ , where some singularities disappear. Other deformations of interest, giving smooth surfaces, are obtained by varying  $\mu$ .

### 3. Cohomology Groups of Tiling Spaces with Ninefold Symmetry

The tiling spaces  $\Omega_X$  are formed by the closure of the translational orbit of one tiling  $X$ . A substitution  $\sigma$  is said to force the border [13] if there is a positive integer  $n$  such that if  $t_1$  and  $t_2$  are two tiles of the same type, then the two level- $n$  supertiles  $\sigma^n(t_1)$  and  $\sigma^n(t_2)$  have, up

to translation, the same pattern of neighboring tiles. If a substitution forces the border, then the tiling space is the inverse limit of the Anderson-Putnam complex  $\Gamma_0$ , which contains one copy of every kind of tile that is allowed with some edges identified [1]. For 2D tiling spaces the cohomology classes are generated by the vertices, edges, and faces of  $\Gamma_0$ .

In addition to  $\Omega_X$  we consider also another type of tiling spaces  $\overline{\Omega}_X$ . The finite rotation group  $\mathbf{Z}_N$  associated to the tiling acts on  $\Omega_X$ , and the quotient  $\Omega_X/\mathbf{Z}_N$  yields the space  $\overline{\Omega}_X$  of tilings modulo a rotation about the origin [14].

We study first the cohomology of a ninefold symmetry tiling space  $\Omega_N$ . The substitution rules for this and other composite patterns were studied in [9]. They can be obtained by using  $S_B$  in Figure 2(b). Up to mirror reflection and rotation, the tiling has three triangular prototiles  $\mathcal{T}$  with inflation or substitution rules (level-1 supertiles) given in Figure 3. Iteration of the inflation rules shows that the tiling has 18 vertex configurations. After three inflation steps, they are transformed into just two vertex configurations that we call  $a$  and  $b$  representing a threefold and a ninefold star, respectively (Figure 4). The substitution forces the border in four steps. The analysis of the vertex sequences appearing in the level-4 superedges shows that there are four edge types  $\alpha_{b,a}, \beta_{a,b}, \gamma_{a,a}, \delta_{b,a}$ , where the subindexes denote the vertices appearing on the edge borders. The lengths of  $\alpha, \beta, \gamma, \delta$  are  $s_1, s_2, s_3, s_4$ , with  $s_v \equiv \sin(v\pi/9)$ .

The rotation group  $\mathbf{Z}_9$  acts freely on edges and tiles. The two vertices satisfy  $a = r^3 a, b = r b$  with  $r^9 = 1$ . We have six tile types  $A = \mathcal{T}(r^4 \gamma, r^4 \beta, r^5 \alpha)$ ,  $\tilde{A} = \mathcal{T}(r^4 \gamma, r^3 \alpha, r^5 \beta)$ ,  $B = \mathcal{T}(\delta, r^8 \gamma, r \alpha)$ ,  $\tilde{B} = \mathcal{T}(\delta, r^7 \alpha, \gamma)$ ,  $C = \mathcal{T}(\delta, r^3 \gamma, r^6 \beta)$ ,  $\tilde{C} = \mathcal{T}(\delta, r^3 \beta, r^5 \gamma)$ , and each appears in 9 orientations. The Anderson-Putnam complex  $\Gamma_0$  has Euler characteristic  $\chi = 22$ .

The three irreducible representations of  $\mathbf{Z}_9$  over the integers are the one-dimensional scalar ( $r = 1$ ), a two-dimensional and a six-dimensional representation. The 2D and the 6D representations have  $r$  acting by multiplication on the rings  $\mathcal{R}_1 = \mathbf{Z}[r]/(r^2 + r + 1)$  and  $\mathcal{R}_2 = \mathbf{Z}[r]/(r^6 + r^3 + 1)$ , respectively. In this case the vertex  $b$  appears only in the scalar representation, the vertex  $a$  in the scalar and 2D representations, while the edges and faces appear in all representations. Vertices, edges, and faces form a basis for the spaces of chains  $C_k$  with  $k = 0, 1, 2$ . The boundary maps  $\partial_k : C_{k+1} \mapsto C_k$  for  $k = 0, 1$  are

$$\partial_1 = \begin{pmatrix} r^5 & -r^3 & -r & r^7 & 0 & 0 \\ r^4 & -r^5 & 0 & 0 & r^6 & -r^3 \\ -r^4 & r^4 & -r^8 & 1 & r^3 & -r^5 \\ 0 & 0 & 1 & -1 & 1 & -1 \end{pmatrix} \quad (3.1)$$

in all representations and

$$\partial_0 = \begin{pmatrix} -r^2 & 1 & 0 & -1 \\ 1 & -1 & 0 & 1 \end{pmatrix} \quad (3.2)$$

in the scalar and 2D representations, but with appropriate modification having in mind that only the vertex  $a$  appears in the 2D representation. If the cochain groups are denoted by  $C^k$ , then, for  $k = 0, 1$ , the coboundary maps  $\delta_k : C^k \mapsto C^{k+1}$  are the transposes of the matrices  $\partial_k$  given above with  $r$  replaced with  $r^T = r^{-1}$ .

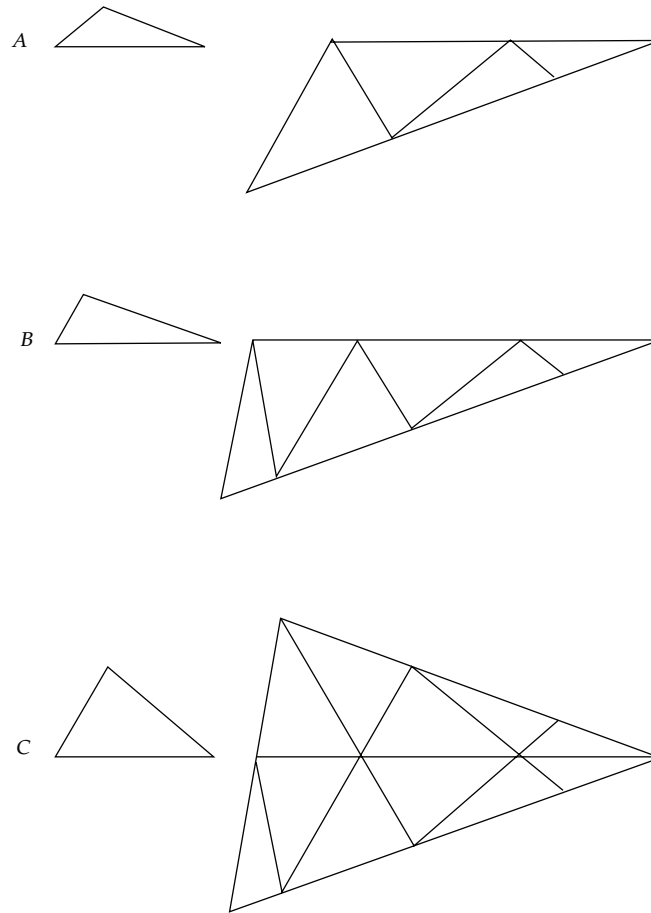


**Figure 3:** Inflation rules for the ninefold symmetry tiling.

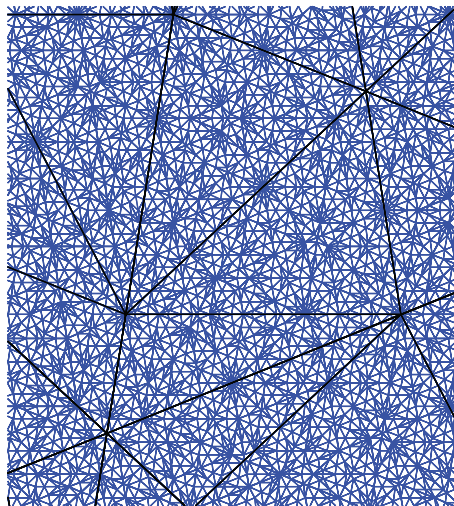


**Figure 4:** Level-3 supertiles in the ninefold symmetry tiling.

*Scalar Representation  $r = 1$* 

In the scalar representation,  $C^0 = \mathbf{Z}^2$ ,  $C^1 = \mathbf{Z}^4$ ,  $C^2 = \mathbf{Z}^6$ . We have  $\text{rank } \delta_0 = 1$  and  $\text{rank } \delta_1 = 3$ . The cohomologies of  $\Gamma_0$  in this representation are  $\mathcal{H}^0 = \text{Ker } \delta_0 = \mathbf{Z}$ ,  $\mathcal{H}^1 = \text{Ker } \delta_1 / \text{Im } \delta_0 = 0$ , and  $\mathcal{H}^2 = \mathbf{Z}^6 / \text{Im } \delta_1 = \mathbf{Z}^3$ .

*2D Representation*

There is one vertex in the 2D representation, and  $C^0, C^1, C^2$  are free modules of dimensions 1, 4, 6 over the ring  $\mathcal{R}_1$ . The rank of  $\delta_0$  over  $\mathcal{R}_1$  is 1, the matrix  $\delta_1$  has rank 3 over  $\mathcal{R}_1$ , and, as abelian groups, we have  $\mathcal{H}^0 = \mathcal{H}^1 = 0, \mathcal{H}^2 = \mathbf{Z}^6$ .

*6D Representation*

There are no vertices in the 6D representation, and  $C^1, C^2$  are free modules of dimensions 1 and 3 over the ring  $\mathcal{R}_2$ . The map  $\delta_1$  has rank 3 over  $\mathcal{R}_2$  and  $\mathcal{H}^0 = 0, \mathcal{H}^1 = \mathbf{Z}^6, \mathcal{H}^2 = \mathbf{Z}^{18}$ .

We have obtained the cohomology of the complex  $\Gamma_0$  which is enough because the tiling forces the border [1]. To get the cohomology of the tiling space  $\Omega_N$ , we need to compute the direct limit of the cohomologies under the substitution.

The substitution matrix on vertices is

$$\sigma_0 = \begin{pmatrix} r^2 & 0 \\ 0 & 1 \end{pmatrix}, \quad (3.3)$$

while the matrix on 1-chains is

$$\sigma_1 = \begin{pmatrix} 0 & 0 & 0 & 1 \\ 0 & 0 & r & r^5 \\ 0 & 1 & r^5 & 1 \\ r & r^5 & r & r^5 \end{pmatrix}, \quad (3.4)$$

and the substitution on 2-chains

$$\sigma_2 = \begin{pmatrix} 0 & r & 0 & r & 1 & r \\ 1 & 0 & 1 & 0 & 1 & r \\ 0 & r^5 & 0 & r^5 + r^8 & r^4 & r^5 + r^8 \\ r^5 & 0 & r^2 + r^5 & 0 & r^2 + r^5 & r^6 \\ r^6 & r & r^6 & r + r^4 & 1 + r^3 + r^6 & r + r^4 + r^7 \\ 1 & r^4 & 1 + r^6 & r^4 & 1 + r^3 + r^6 & r + r^4 + r^7 \end{pmatrix}. \quad (3.5)$$

The induced matrices on cochains  $\sigma_k^*$  are obtained by transposition of the matrices  $\sigma_k$  with  $r$  replaced with  $r^{-1}$ . They are isomorphisms, and the direct limit of each  $\mathcal{H}^k$  is simply  $\mathcal{H}^k$ . By taking into account all the irreducible representations, we get the following

$$\mathcal{H}^0(\Omega_N) = \mathbf{Z}, \quad \mathcal{H}^1(\Omega_N) = \mathbf{Z}^6, \quad \mathcal{H}^2(\Omega_N) = \mathbf{Z}^{27}. \quad (3.6)$$

The cohomology of  $\overline{\Omega}_X$  is the rotationally invariant part of the cohomology of  $\Omega_X$ , and we have

$$\mathcal{H}^0(\overline{\Omega}_N) = \mathbf{Z}, \quad \mathcal{H}^1(\overline{\Omega}_N) = 0, \quad \mathcal{H}^2(\overline{\Omega}_N) = \mathbf{Z}^3. \quad (3.7)$$

Another tiling space with noncrystallographic symmetries and vanishing first cohomology in  $\overline{\Omega}_X$  was analyzed in [6]. The pentagonal tiling space  $\Omega_{\Xi_+}$  has the same prototiles as the Robinson decomposition of the Penrose tilings:  $A, B$  with edges  $\alpha, \beta$  and lengths  $s_1, s_2$ , with  $s_\nu \equiv \sin(\nu\pi/5)$ . The inflation rules can be obtained from  $S_B$  in Figure 1(a) with arrows as indicated in [6]. The cohomology groups are

$$\mathcal{H}^0(\Omega_{\Xi_+}) = \mathbf{Z}, \quad \mathcal{H}^1(\Omega_{\Xi_+}) = \mathbf{Z}^4, \quad \mathcal{H}^2(\Omega_{\Xi_+}) = \mathbf{Z}^{14}, \quad (3.8)$$

and the rotationally invariant part is  $\mathcal{H}^0(\overline{\Omega}_{\Xi_+}) = \mathbf{Z}$ ,  $\mathcal{H}^1(\overline{\Omega}_{\Xi_+}) = 0$ ,  $\mathcal{H}^2(\overline{\Omega}_{\Xi_+}) = \mathbf{Z}^2$ .

Fractal tilings related with Penrose patterns have been studied in [15, 16]. In addition to the computation of the cohomologies, the analysis of the patterns of vertex configurations, appearing in  $\Xi_+$  on the level-6 superedges, can be used also to construct tilings whose edges and tiles have irregular shapes. In Figure 5(a) we have shown the vertex sequences arising in the  $A$ -type level-6 supertile (see Figure 12 in [6]). The borders of the new prototile shapes are formed by concatenation of scaled copies of oriented  $\alpha$  and  $\beta$ . The substitution rules for the corresponding pattern can be seen in Figure 5(b).

Tiling spaces with crystallographic symmetries also may have zero first cohomology. For instance the chair tiling space  $\Omega_{\text{CH}}$  has [14]

$$\mathcal{H}^0(\Omega_{\text{CH}}) = \mathbf{Z}, \quad \mathcal{H}^1(\Omega_{\text{CH}}) = \mathbf{Z} \left[ \frac{1}{2} \right]^2, \quad \mathcal{H}^2(\Omega_{\text{CH}}) = \mathbf{Z} \left[ \frac{1}{4} \right] \oplus \mathbf{Z} \left[ \frac{1}{2} \right]^2 \quad (3.9)$$

with  $\mathcal{H}^0(\overline{\Omega}_{\text{CH}}) = \mathbf{Z}$ ,  $\mathcal{H}^1(\overline{\Omega}_{\text{CH}}) = 0$ ,  $\mathcal{H}^2(\overline{\Omega}_{\text{CH}}) = \mathbf{Z}[1/4]$ . In the next section we study other tiling spaces with crystallographic symmetries, which also have  $\mathcal{H}^1(\overline{\Omega}_T) = 0$ .

## 4. Tiling Spaces with Threefold Symmetry

### 4.1. Equithirds Tiling

The equithirds tiling was obtained independently by L. Danzer and B. Kalahurka ([5] and references therein). It is based on the substitution of Figure 6. The prototiles are an equilateral triangle of side length 1 and an isosceles triangle with sides of length 1, 1, and  $\sqrt{3}$ .



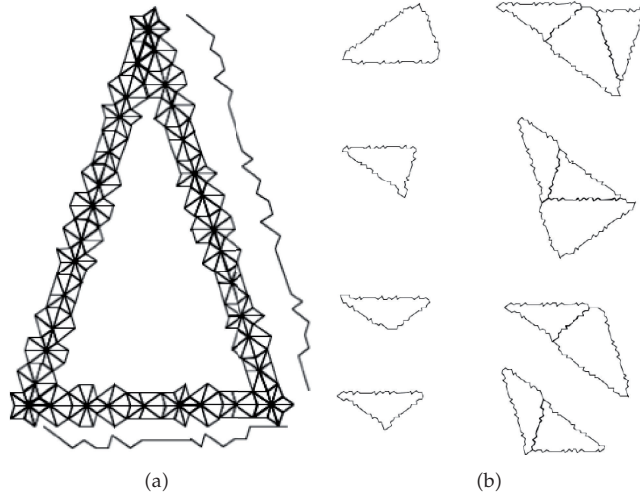


Figure 5: Pentagonal tiling with irregular shapes: (a) construction of the boundaries, (b) inflation rules.

The analysis of the five vertex configurations shows that, after one inflation step, they are transformed into one: vertex  $a$ . The substitution forces the border in two steps. We denote the edges by  $\alpha, \beta$  with lengths  $1, \sqrt{3}$ , and the rotation group  $\mathbf{Z}_3$  acts freely on them.

We have four tile types  $A = \mathcal{T}(\alpha, r\alpha, r^2\alpha)$ ,  $\bar{A} = \mathcal{T}(\alpha, r\alpha, r^2\alpha)$ ,  $B = \mathcal{T}(\alpha, \beta, r\alpha)$ ,  $\bar{B} = \mathcal{T}(\alpha, r^2\alpha, r^2\beta)$ , with  $r^3 = 1$ . The tiles  $B, \bar{B}$  appear in three orientations and  $A, \bar{A}$  in one. The Anderson-Putnam complex  $\Gamma_0$  has therefore Euler characteristic  $\chi = 3$ .

The two irreducible representations of  $\mathbf{Z}_3$  over the integers are the one-dimensional scalar ( $r = 1$ ) and a two-dimensional vector representation. The vector representation has  $r$  acting by multiplication on the ring  $\mathcal{R}_1 = \mathbf{Z}[r]/(r^2 + r + 1)$ . The edges and the tiles  $B, \bar{B}, D$  appear in all representations, while the vertex and the tiles  $A, \bar{A}$  appear only in the scalar representation. The boundary maps are  $\partial_0 = 0$  and

$$\partial_1 = \begin{pmatrix} 1 & -1 & 1-r & 1-r^2 \\ 0 & 0 & -1 & r^2 \end{pmatrix}. \tag{4.1}$$

### Scalar Representation $r = 1$

In the scalar representation,  $C^0 = \mathbf{Z}$ ,  $C^1 = \mathbf{Z}^2$ ,  $C^2 = \mathbf{Z}^4$ . In this case  $\text{rank } \delta_1 = 2$  and we have  $\mathcal{H}^0 = \text{Ker } \delta_0 = \mathbf{Z}$ ,  $\mathcal{H}^1 = \text{Ker } \delta_1 / \text{Im } \delta_0 = 0$ , and  $\mathcal{H}^2 = \mathbf{Z}^4 / \text{Im } \delta_1 = \mathbf{Z}^2$ .

### Vector Representation

There are two tiles in the 2D representation, and  $C^1, C^2$  are free modules of dimensions 2 over the ring  $\mathcal{R}_1$ . The rank of  $\delta_1$  over  $\mathcal{R}_1$  is 1 and we have  $\mathcal{H}^0 = 0$ ,  $\mathcal{H}^1 = \mathbf{Z}^2$  and  $\mathcal{H}^2 = \mathbf{Z}^2$ .

The cohomology of the complex  $\Gamma_0$  is therefore  $\mathcal{H}^0(\Gamma_0) = \mathbf{Z}$ ,  $\mathcal{H}^1(\Gamma_0) = \mathbf{Z}^2$  and  $\mathcal{H}^2(\Gamma_0) = \mathbf{Z}^4$ . Now we compute the direct limit of the cohomologies under the substitution.

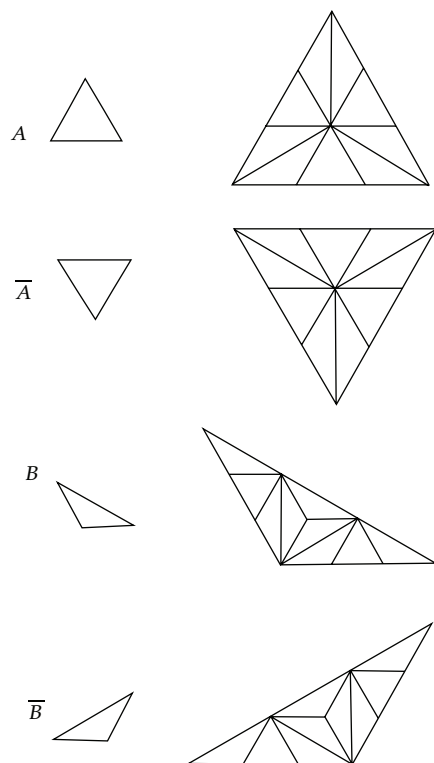


Figure 6: Inflation rules for the equithirds tiling.

The substitution on the vertex is the identity. The substitution on edges is represented by

$$\sigma_1 = \begin{pmatrix} 3 & 0 \\ 0 & 3 \end{pmatrix}, \quad (4.2)$$

and the substitution on 2-chains is

$$\sigma_2 = \begin{pmatrix} 3 & 0 & 1 & 1 \\ 0 & 3 & 1 & 1 \\ 1+r+r^2 & 1+r+r^2 & 3+r+r^2 & 1+r \\ 1+r+r^2 & 1+r+r^2 & 1+r^2 & 3+r+r^2 \end{pmatrix}. \quad (4.3)$$

In the scalar representation the direct limits of each  $\mathcal{L}^k$ , under the action of the induced matrices on cochains  $\sigma_k^*$ , are  $\mathcal{L}^k$  for  $k = 0, 1$ . We can take a basis for  $\mathcal{L}^2$  in terms of the canonical basis of  $\mathbf{Z}^4$  formed by  $e_1, e_1 + e_3$  with the classes of  $v_3 = e_4 - e_3$ ,  $v_4 = e_2 - e_1$  cohomologous to zero. The eigenvalues of  $\sigma_2^*$  are 9, 3, 1 with eigenvectors  $v_1 = (1, 1, 1, 1)^T$ ,  $v_2, v_3, v_4 = (-3, -3, 1, 1)^T$ . Its action on  $\mathcal{L}^2$  gives the direct limit  $\mathbf{Z} \oplus \mathbf{Z}[1/3]$ .

In the vector representation the direct limit of  $\mathcal{L}^1$  is  $\mathbf{Z}[1/3]^2$ . A base for  $\mathcal{L}^2$  in this representation is given by the vector  $(-1, 0)^T \sim (r, 1)^T$  which is the eigenvector of  $\sigma_2^*$  with

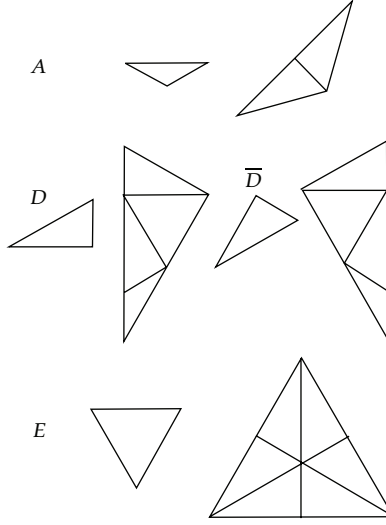


Figure 7: Inflation rules for  $T$ .

eigenvalue 1. The direct limit is now  $\mathbf{Z}^2$ . The cohomology groups for the equithirds tiling space  $\Omega_{\text{EQ}}$  are (see also [5])

$$\check{\mathcal{H}}^0(\Omega_{\text{EQ}}) = \mathbf{Z}, \quad \check{\mathcal{H}}^1(\Omega_{\text{EQ}}) = \mathbf{Z} \left[ \frac{1}{3} \right]^2, \quad \check{\mathcal{H}}^2(\Omega_{\text{EQ}}) = \mathbf{Z}^3 \oplus \mathbf{Z} \left[ \frac{1}{3} \right]. \quad (4.4)$$

The rotationally invariant part of the cohomology is

$$\check{\mathcal{H}}^0(\overline{\Omega}_{\text{EQ}}) = \mathbf{Z}, \quad \check{\mathcal{H}}^1(\overline{\Omega}_{\text{EQ}}) = 0, \quad \check{\mathcal{H}}^2(\overline{\Omega}_{\text{EQ}}) = \mathbf{Z} \oplus \mathbf{Z} \left[ \frac{1}{3} \right]. \quad (4.5)$$

#### 4.2. The Tiling Spaces $\Omega_T$

Although the paper [7] deals with tilings having odd symmetries nondivisible by three, the authors consider a case which can be derived with a set of six lines in the plane. The tiling spaces  $\Omega_T$  that we treat now are based on such system of lines. In the construction discussed in Section 2, it corresponds to the simplicial arrangements  $S_A; S_C$  in Figure 1(b).

The substitution rules for  $T$  are represented in Figure 7, and its seven vertex configurations can be seen in Figure 8. After two inflation steps the vertex configurations are transformed into the configurations 1 and 2 which are denoted by  $a, b$ . The substitution forces the border also in two steps: the vertex sequences in the level-2 superedges (Figure 9) are  $\alpha : 53, \beta : 67\bar{6}, \gamma : 2354$  with lengths  $s_1, s_2, s_3, s_v \equiv \sin(v\pi/6)$ , and the vertices in the edge borders are  $\alpha : ab, \beta : aa, \gamma : ab$ . The rotation group  $\mathbf{Z}_3$  acts freely on the edges and  $a = ra, b = rb$  with  $r^3 = 1$ .

The four tile types are  $A = \mathcal{T}(\alpha, r^2\alpha, \beta), D = \mathcal{T}(\beta, r\alpha, \gamma), \bar{D} = \mathcal{T}(\gamma, \alpha, r^2\beta),$  and  $E = \mathcal{T}(\beta, r\beta, r^2\beta),$  and each appears in 3 orientations, except  $E$  which appears in only one. The Euler characteristic of  $\Gamma_0$  is  $\chi = 3$ .

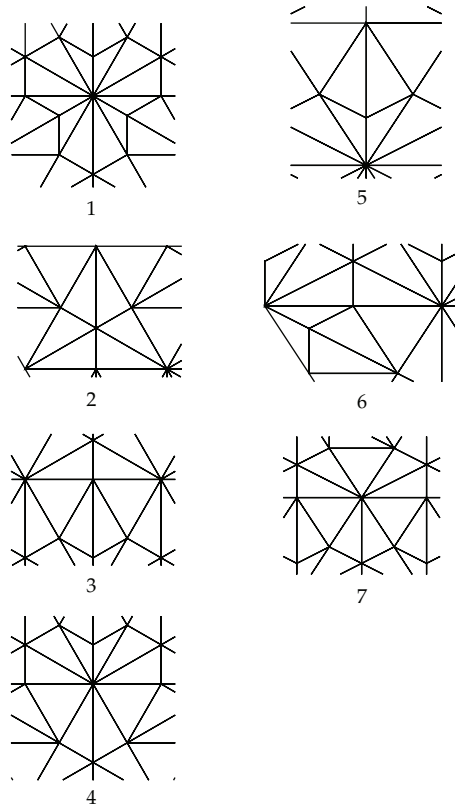


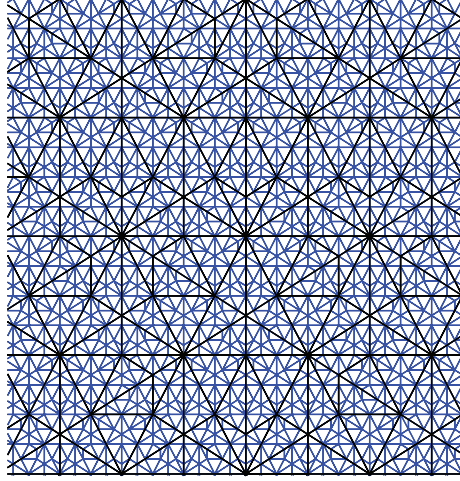
Figure 8: Vertex configurations in  $T$ .

In this case the edges and the tiles  $A, D, \bar{D}$  appear in all representations of  $\mathbf{Z}_3$ , while the vertices  $a, b$ , and the tile  $E$  appear only in the scalar representation. The boundary maps are

$$\begin{aligned} \partial_0 &= \begin{pmatrix} -1 & 0 & -1 \\ 1 & 0 & 1 \end{pmatrix}, \\ \partial_1 &= \begin{pmatrix} 1-r^2 & r & -1 & 0 \\ -1 & 1 & r^2 & -1 \\ 0 & -1 & 1 & 0 \end{pmatrix}. \end{aligned} \tag{4.6}$$

#### Scalar Representation $r = 1$

In this representation,  $C^0 = \mathbf{Z}^2$ ,  $C^1 = \mathbf{Z}^3$ ,  $C^2 = \mathbf{Z}^4$ . Here  $\text{rank } \delta_0 = 1$  and  $\text{rank } \delta_1 = 2$  with cohomologies  $\mathcal{H}^0 = \text{Ker } \delta_0 = \mathbf{Z}$ ,  $\mathcal{H}^1 = \text{Ker } \delta_1 / \text{Im } \delta_0 = 0$  and  $\mathcal{H}^2 = \mathbf{Z}^4 / \text{Im } \delta_1 = \mathbf{Z}^2$ .

Figure 9: Level-2 supertiles in  $T$ .

### Vector Representation

There are three edges and three tiles in the 2D representation, and  $C^1, C^2$  are free modules of dimension 3 over the ring  $\mathcal{R}_1$ . The rank of  $\delta_1$  over  $\mathcal{R}_1$  is 2, and, as abelian groups, we have  $\mathcal{H}^0 = 0$ ,  $\mathcal{H}^1 = \mathbf{Z}^2$  and  $\mathcal{H}^2 = \mathbf{Z}^2$ .

Adding up the contributions of each representations, we get the cohomology of the complex  $\Gamma_0$ :  $\mathcal{H}^0(\Gamma_0) = \mathbf{Z}$ ,  $\mathcal{H}^1(\Gamma_0) = \mathbf{Z}^2$ , and  $\mathcal{H}^2(\Gamma_0) = \mathbf{Z}^4$ .

The substitution on the vertices is the  $2 \times 2$  identity matrix. The substitution on 1-chains is

$$\sigma_1 = \begin{pmatrix} 0 & 0 & 2r \\ 0 & 2r^2 & 0 \\ 1 & 0 & r^2 \end{pmatrix}, \quad (4.7)$$

and the substitution on 2-chains is

$$\sigma_2 = \begin{pmatrix} 0 & r^2 & r & 0 \\ r^2 & 0 & 1+r^2 & 1 \\ 1 & r+r^2 & 0 & 1 \\ 0 & 1 & 1 & 0 \end{pmatrix}. \quad (4.8)$$

In the scalar representation the direct limits of  $\mathcal{H}^k$  for  $k = 0, 1$  are  $\mathcal{H}^k$ . A base for  $\mathcal{H}^2$  in this representation is given by the vectors  $u_3 = (0, 0, 1, 0)^T$ ,  $u_4 = (0, 0, 0, 1)^T$ , and the classes of  $u_k, k = 1, 2$ , with  $u_1 = (0, 1, -1, 0)^T$ ,  $u_2 = (-1, 0, 2, -1)^T$ , are cohomologous to zero. The action of  $\sigma_2^*$  applied twice to  $u_3$  gives  $4u_3 \sim 4u_4$ , and the direct limit yields a contribution of  $\mathbf{Z}[1/2]$ .

In the vector representation  $v_3 = (1, 1-r, -2r)^T$  forms a base for  $\mathcal{H}^1$ . The matrix  $\sigma_1^*$  has eigenvalues  $-r, 2r, 2r$  with eigenvectors  $(-r^2, 0, 1)^T, (r^2, 0, 2)^T, (0, 1, 0)^T$ , and the direct sum of

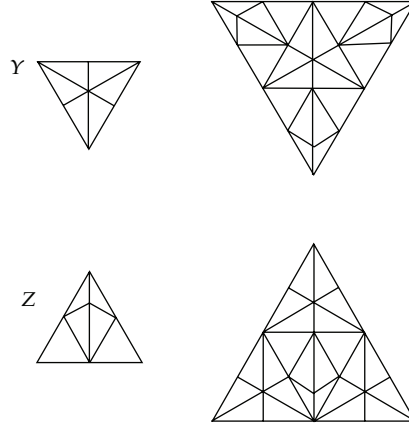


Figure 10: Inflation rules for the patches  $Y$  and  $Z$  in  $T$ .

the eigenspaces is not isomorphic to all  $\mathbf{Z}^6$ . The action of  $\sigma_1^*$  gives a contribution of  $\mathbf{Z}[1/2]^2$  to the first cohomology. A base for  $\mathcal{H}^2$  is given by  $u_3 = (0, 1, 0)^T$  with  $u_1 = (1 - r, r^2, 1)^T$ ,  $u_2 = (-1, -r^2, 0)^T$  cohomologous to zero. We have  $\sigma_1^{*3}u_3 \sim u_3$ , and the direct limit of  $\mathcal{H}^2$  is  $\mathbf{Z}^2$ . The cohomology groups are then

$$\check{\mathcal{H}}^0(\Omega_T) = \mathbf{Z}, \quad \check{\mathcal{H}}^1(\Omega_T) = \mathbf{Z} \left[ \frac{1}{2} \right]^2, \quad \check{\mathcal{H}}^2(\Omega_T) = \mathbf{Z}^2 \oplus \mathbf{Z} \left[ \frac{1}{2} \right]. \tag{4.9}$$

The rotationally invariant part of the cohomology is

$$\check{\mathcal{H}}^0(\overline{\Omega}_T) = \mathbf{Z}, \quad \check{\mathcal{H}}^1(\overline{\Omega}_T) = 0, \quad \check{\mathcal{H}}^2(\overline{\Omega}_T) = \mathbf{Z} \left[ \frac{1}{2} \right]. \tag{4.10}$$

With the purpose of studying the meaning of the topological invariants in tiling spaces, Sadun shows that there are patches in the equithirds tiling that play a role analogous to return words in one dimension [5]. The control patches are the equilateral triangle and a rhombus, formed by two isosceles triangles, in three different orientations. This case illustrates the more general property that if the rank of the second rational cohomology is  $k$ , then the number of control patches is also  $k$ . The number of appearances of any patch in a sufficiently substituted rhombus in the equithirds tiling is then determined by the number of appearances of the four control patches.

For the tiling  $T$  we may find four patches that generate the tilings, because they obey certain substitution rules induced by the inflation on the triangular prototiles. The patches  $Y, Z$ , and their substitution rules are represented in Figure 10. The patch content in the inflation rules is

$$Y \mapsto YZ\overline{Z}\overline{\overline{Z}} \quad Z \mapsto \overline{Z}Y\overline{Y}Y, \tag{4.11}$$

where  $\overline{Z}$  and  $\overline{\overline{Z}}$  represent rotated versions of  $Z$  by 120 and 240 degrees.

Although we have studied in detail only some particular cases, we can see that the general constructions of substitutions proposed in [7, 8] are a rich source of tiling spaces with unusual properties. The tilings with noncrystallographic symmetries studied in this paper, derived with such constructions, have vanishing rotationally invariant first cohomology, but this is not true in general. For instance, the analysis of a tiling  $T^*$  obtained with the same basic construction as  $T$  (which has inflation factor  $s_3/s_1$ ) but with scaling factor  $s_2/s_1$  shows that the associated tiling space has in  $\mathcal{L}^1$  a nontrivial rotationally invariant piece. The tiling  $T^*$  has six prototiles with the same three shapes  $A, D, E$  as in  $T$ . The mirror images of  $A, D$ , and  $E$  shape level-1 supertiles are different in  $T^*$ , while in  $T$  we have two mirror inflation rules only for  $D$  (Figure 7). The first cohomology for the tiling space  $\Omega_{T^*}$  in the scalar representation of  $\mathbf{Z}_3$  is now  $\mathbf{Z}$ . An open question is, for general tiling spaces, which property distinguishes them in relation to the existence of a nontrivial rotationally invariant component in the first cohomology group.

## References

- [1] J. E. Anderson and I. F. Putnam, "Topological invariants for substitution tilings and their associated  $C^*$ -algebras," *Ergodic Theory and Dynamical Systems*, vol. 18, no. 3, pp. 509–537, 1998.
- [2] N. P. Frank and L. Sadun, "Fusion: a general framework for hierarchical tilings of  $\mathbb{R}^d$ ," In press, <http://arxiv.org/abs/1101.4930>.
- [3] J. Kellendonk and I. F. Putnam, "The Ruelle-Sullivan map for actions of  $\mathbb{R}^n$ ," *Mathematische Annalen*, vol. 334, no. 3, pp. 693–711, 2006.
- [4] M. Barge, H. Bruin, L. Jones, and L. Sadun, "Homological Pisot substitutions and exact regularity," *Israel Journal of Mathematics*. In press, <http://arxiv.org/abs/1001.2027>.
- [5] L. Sadun, "Exact regularity and the cohomology of tiling spaces," *Ergodic Theory and Dynamical Systems*, vol. 31, pp. 1819–1834, 2011.
- [6] J. G. Escudero, "Randomness and topological invariants in pentagonal tiling spaces," *Discrete Dynamics in Nature and Society*, vol. 2011, Article ID 946913, 23 pages, 2011.
- [7] K.-P. Nischke and L. Danzer, "A construction of inflation rules based on  $n$ -fold symmetry," *Discrete & Computational Geometry*, vol. 15, no. 2, pp. 221–236, 1996.
- [8] J. G. Escudero, "Random tilings of spherical 3-manifolds," *Journal of Geometry and Physics*, vol. 58, no. 11, pp. 1451–1464, 2008.
- [9] J. G. Escudero, "Composition of inflation rules for aperiodic structures with nine-fold symmetry," *International Journal of Modern Physics B*, vol. 13, no. 4, pp. 363–373, 1999.
- [10] J. G. Escudero, "A construction of algebraic surfaces with many real nodes," In press, <http://arxiv.org/abs/1107.3401>.
- [11] S. V. Chmutov, "Examples of projective surfaces with many singularities," *Journal of Algebraic Geometry*, vol. 1, no. 2, pp. 191–196, 1992.
- [12] S. Breske, O. Labs, and D. van Straten, "Real line arrangements and surfaces with many real nodes," in *Geometric Modeling and Algebraic Geometry*, pp. 47–54, Springer, Berlin, Germany, 2008.
- [13] J. Kellendonk, "Noncommutative geometry of tilings and gap labelling," *Reviews in Mathematical Physics*, vol. 7, no. 7, pp. 1133–1180, 1995.
- [14] L. Sadun, *Topology of Tiling Spaces*, vol. 46 of *University Lecture Series*, American Mathematical Society, Providence, RI, USA, 2008.
- [15] C. Bandt and P. Gummelt, "Fractal Penrose tilings. I. Construction and matching rules," *Aequationes Mathematicae*, vol. 53, no. 3, pp. 295–307, 1997.
- [16] G. Gelbrich, "Fractal Penrose tiles. II. Tiles with fractal boundary as duals of Penrose triangles," *Aequationes Mathematicae*, vol. 54, no. 1-2, pp. 108–116, 1997.





# Hindawi

Submit your manuscripts at  
<http://www.hindawi.com>

